WASTEWATER TREATMENT • RESEARCH ARTICLE

Preparation of calcium oxalate—bromopyrogallol red inclusion sorbent and application to treatment of cationic dye and heavy metal wastewaters

Hong-Yan Wang · Hong-Wen Gao

Abstract

Background, aim, and scope Dye pollutants are a major class of environmental contaminants. Over 100,000 dyes have been synthesized worldwide and more than 700,000 tons are produced annually and over 5% are discharged into aquatic environments. The adsorption or sorption is one of the most efficient methods to remove dye and heavy metal pollutants from wastewater. However, most of the present sorbents often bear some disadvantages, e.g. low sorption capacity, difficult separation of spoil, complex reproduction, or secondary pollution. Development of novel sorbents that can overcome these limitations is desirable.

Materials and methods On the basis of the chemical coprecipitation of calcium oxalate (CaC_2O_4), bromopyrogallol red (BPR) was embedded during the growing of CaC_2O_4 particles. The ternary $C_2O_4^{2-}$–BPR–Ca^{2+} sorbent was yielded by the centrifugation. Its composition was determined by spectrophotometry and AAS, and its structure and morphology were characterized by powder X-ray diffraction (XRD), laser particle-size analysis, and scanning electron microscopy (SEM). The adsorption of ethyl violet (EV) and heavy metals, e.g. Cu(II), Cd(II), Ni (II), Zn(II), and Pb(II) were carried out and their removal

rate determined by spectrophotometry and ICP-OES. The adsorption performance of the sorbent was compared with powder activated carbon. The Langmuir isothermal model was applied to fit the embedment of BPR and adsorption of EV.

Results The saturation number of BPR binding to CaC_2O_4 reached 0.0105 mol/mol and the adsorption constant of the complex was 4.70×10^5 M^{-1}. Over 80% of the sorbent particles are between 0.7 and 1.02 μm, formed by the aggregation of the global CaC_2O_4/BPR inclusion grains of 30–50 nm size. Such a material was found to adsorb cationic dyes selectively and sensitively. Ethyl violet (EV) was used to investigate the adsorption mechanism of the material. One BPR molecule may just bind with one EV molecule. The CaC_2O_4/BPR inclusion material adsorbed EV over two times more efficiently than the activated carbon. The adsorption of EV on the CaC_2O_4/BPR inclusion sorbent was complete in only 5 min and the sedimentation complete in 1 h. However, those of EV onto activated carbon took more than 1.5 and 5 h, respectively. The treatment of methylene blue and malachite green dye wastewaters indicated that only 0.4% of the sorbent adsorbed over 80% of color substances. Besides, the material can also adsorb heavy metals by complexation with BPR. Over 90% of Pb^{2+}, and approximately 50% of Cd^{2+} and Cu^{2+}, were removed in a high Zn^{2+}-electroplating wastewater when 3% of the material was added. Eighty-six percent of Cu^{2+}, and 60% of Ni^{2+} and Cd^{2+}, were removed in a high Cd^{2+}-electroplating wastewater.

Discussion The embedment of BPR into CaC_2O_4 particles responded to the Langmuir isothermal adsorption. As the affinity ligand of Ca^{2+}, BPR with sulfonic groups may be adsorbed into the temporary electric double layer during the growing of CaC_2O_4 particles. Immediately, $C_2O_4^{2-}$ captured the Ca^{2+} to form the CaC_2O_4 outer enclosed sphere.

H.-Y. Wang · H.-W. Gao (✉)
State Key Laboratory of Pollution Control and Resource Reuse,
College of Environmental Science and Engineering,
Tongji University,
Shanghai 200092, China
e-mail: hwgao@tongji.edu.cn

Thus, BPR may be released and embedded as a sandwich between CaC_2O_4 layers. The adsorption of EV on the sorbent obeyed the Langmuir isothermal equation and adsorption is mainly due to the ion-pair attraction between EV and BPR. Different from the inclusion sorbent, the activated carbon depended on the specific surface area to adsorb organic substances. Therefore, the adsorption capacity, equilibrium, and sedimentation time of the sorbent are much better than activated carbon. The interaction of heavy metals with the inclusion sorbent responded to their coordination.

Conclusions By characterizing the $C_2O_4^{2-}$–BPR–Ca^{2+} inclusion material using various modern instruments, the ternary in situ embedment particle, $[(CaC_2O_4)_{95}(BPR)]_n^{2n-}$, an electronegative, micron-sized adsorbent was synthesized. It is selective, rapid, and highly effective for adsorbing cationic dyes and heavy metals. Moreover, the adsorption is hardly subject to the impact of electrolytes.

Recommendations and perspectives The present work provides a simple and valuable method for preparing the highly effective adsorbent. If a concentrated BPR wastewater was reused as the inclusion reactant, the sorbent will be low cost. By selecting the inclusion ligand with a special structure, we may prepare some particular functional materials to recover the valuable substances from seriously polluted wastewaters. The recommended method will play a significant role in development of advanced adsorption materials.

Keywords Calcium oxalate · Bromopyrogallol red · Chemical coprecipitation · Dyes · Heavy metals · Inclusion sorbent · Sorbents · Wastewater treatment

1 Background, aim, and scope

Chemical pollutants continuously released from various sources raise a number of ecological concerns because their biodegradation is normally very slow and conventional treatments are either ineffective or non-environmentally compatible (Chatterjee and Dasgupta 2005). Dye pollutants are a major class of environmental contaminants. Over 100,000 dyes have been synthesized worldwide and more than 700,000 tons are produced annually (McMullan et al. 2001). More than 10,000 dyes are commercially available and over 5% are discharged into aquatic environments by textile industries (Gong et al. 2005). Dye wastewaters are highly resistant to light, heat, oxidation agents, and biodegradation because dyestuffs are often synthetic aromatic compounds containing a variety of functional groups. Some dyes are reported to cause allergy, dermatitis, skin irritation, cancer, and mutations in humans (Sudipta et al. 2005; Maloney et al. 2000). Thus, it is critical to remove

dyes from wastewaters before they are discharged to effluent-receiving water bodies.

The conventional treatments of dye wastewaters mainly include physical, chemical, and biological methods (Moosvi et al. 2007; Li and Xi 2004). Physico-chemical processes are commonly used to treat dye-laden wastewater. These processes encompass flocculation, electroflotation, precipitation, electro-kinetic coagulation, ion exchange, membrane filtration, electrochemical destruction, and irradiation (Noroozi et al. 2007). The coagulative precipitation with aluminium or iron salts is a classical methodology, but its removal efficiency is poor for dye contaminants. The dye-oxidating method, e.g. using Fenton agent, has a remarkable color removal capability (Wang et al. 2005), but the resulting degradation by-products may be more toxic. Increasing numbers of novel environmental materials, such as titanium dioxide photocatalyst, are being developed for removing organic dyes (Senthilkumaar and Porkodi 2005; Donlagic and Levec 1998). The electrochemical method (may insert one or two advantages of this method here before talking about its demerits) has to consume plenty of energy to reach a satisfactory removal of dye (Jiang et al. 2006). In general, all the processes above are costly and cannot be used by small industries to treat a wide range of dye wastewaters (Mall et al. 2005). The adsorption or sorption is one of the most efficient methods to remove dye and heavy metal pollutants from wastewater (González et al. 2008; Chen et al. 2007). Sorbents may be of natural, mineral, organic, or biological origin (Janos 2003). For example, activated carbon has been used most commonly (Mohanty et al. 2006; Kadirvelu et al. 2005), but its cost is relatively high (Van der Zee et al. 2003). Bentonite as a natural sorbent is widely studied and a great deal of surfactant-modified bentonite materials have been prepared for the treatment of organic dye wastewaters (Wolfe et al. 1986). However, the desorption of surfactant from bentonite does not decrease the chemical oxygen demand (COD) (Zhu et al. 1995). Waste materials, such as shells, husks, plant leaves, sewage sludge-amended soil, and wood sawdust were tested as sorbents of organic substances and heavy metals, too (Yue et al. 2007; Laasri et al. 2007; Mane et al. 2007; Sciban et al. 2007; Antoniadis et al. 2007). However, most of the present sorbents often bear some disadvantages, e.g. low sorption capacity, difficult separation of spoil, complex reproduction, or secondary pollution. Consequently, development of novel sorbents that can overcome these limitations is desirable.

The coprecipitation is often applied to enrichment of metal ions (Tuzen et al. 2008) and synthesis of functional materials (Potapova et al. 2005). In the present work, a commercial dye, bromopyrogallol red (BPR) used as textile dye, pigment additive and a metal-complexing agent (Chen et al. 2003), was selected as the inclusion compound and

the chemical coprecipitation of BPR with CaC_2O_4 investigated to prepare a practical BPR/CaC_2O_4 inclusion material for treatment of cationic dye and heavy metal wastewaters.

2 Materials and methods

2.1 Preparation of the inclusion materials

2.1.1 The addition subsequence of reactants and optimization of Ca^{2+} addition

All studies were carried out in 10.0-ml calibrated flasks in three different subsequences: 1 ethanol–C $C_2O_4^{2-}$–BPR–Ca^{2+}, 2 ethanol–Ca^{2+}–BPR–$C_2O_4^{2-}$, and 3 ethanol–$C_2O_4^{2-}$–Ca^{2+}–BPR. All of these three types of solutions are composed of 40% ethanol, 10.0 μg/ml $C_2O_4^{2-}$, 0.010 μmol/ml BPR, and 200 mg/l Ca^{2+}. The first and second addition sequences were to prepare the BPR/CaC_2O_4 inclusion material and the third sequence to prepare the BPR/CaC_2O_4 surface-modifying material. The absorption spectra of the three solutions were measured by spectrophotometry against the corresponding blank without $C_2O_4^{2-}$. According to the first addition sequence, different concentrations of Ca^{2+} (10.0, 30.0, 50.0, 100, 150, 200, 300, and 500 mg/l) were added into the solutions containing ethanol (40%), $C_2O_4^{2-}$ (10.0 μg/ml), and BPR (0.010 μmol/ml) and their absorption spectra were measured against the reagent blank.

2.1.2 Binding of BPR to CaC_2O_4 particles

In a series of flasks, 40% ethanol, 10.0 μg/ml $C_2O_4^{2-}$, and 0, 1.0, 3.0, 5.0, 10.0, 15.0, 20.0, 25.0, 30.0, 40.0, and 50.0 μmol/l BPR were diluted to approximately 5 ml with deionized water. Ca^{2+}, 200 mg/l, was then added and the mixture was diluted to 10 ml. After reacting for 10 min, the suspending substances were centrifuged for 10 min at 11,000 rpm. The precipitate, i.e. BPR/CaC_2O_4 inclusion material, was prepared. The absorbances of the supernatants were measured at 566 nm and, thus, the unbound BPR (c_L) was determined. According to the third addition sequence, the BPR/CaC_2O_4 surface-modifying material was prepared and the unbound BPR (c_L) was determined as well. Thus, the mole mass of CaC_2O_4 and γ of BPR were calculated. In addition, the effect of electrolyte with concentrations ranging from 0 to 1 M was examined.

2.1.3 Preparation of the inclusion materials with BPR wastewater as a reactant

In order to yield a practical and cost-effective sorbent, BPR wastewater was tested as a reactant in this work. A BPR wastewater sample (pH 5.2, chemical oxygen demand 3,800 mg/l, and BPR 4.5 mmol/l) was collected from a chemical plant and 200 ml of the wastewater was added into one 2,000-ml beaker with 400 ml of ethanol. Four hundred milliliters of 5% $CaCl_2$ was then added and mixed thoroughly by stirring before 100 ml of 1% $Na_2C_2O_4$ was slowly added. The reaction liquid was stewed for precipitating the suspending substances and the precipitate was then washed with 3,000 ml of deionized water three times. The final suspending substance liquid with concentrated CaC_2O_4/BPR inclusion material was used as the product. Ten milliliters of the product liquid was centrifuged, dried, and weighed. The content of the inclusion material in the product liquid was determined. With the same method, the CaC_2O_4/BPR surface-modifying material liquid was also prepared by following the third addition sequence described above.

2.1.4 Composition and size of the materials

Into 10 mg of the CaC_2O_4-only, CaC_2O_4/BPR surface-modifying and CaC_2O_4/BPR inclusion materials, 5 ml of 0.2 mol/l EDTA and 1 ml of 10% triethanolamine were added for dissolving the materials. The solutions were diluted to 50 ml. Ca content was determined by atomic absorption spectrophotometry (AAS) (Scancar et al. 2000). BPR was determined by spectrophotometry at 566 nm and $C_2O_4^{2-}$ at 525 nm with acidic $KMnO_4$ (Hassouna and Elsuccary 2002). In addition, the size distributions of CaC_2O_4-only and CaC_2O_4/BPR inclusion materials were measured with a particle size analyzer. The XRD and SEM images of the CaC_2O_4-only and CaC_2O_4/BPR inclusion materials were acquired to compare their crystallization process, crystal size, and structure.

2.2 Adsorption performance of materials

2.2.1 Adsorption of cationic dyes

Totally, four dye solutions were prepared in this study. Two of them contained anionic dyes: 0.050 mM reactive brilliant red and 0.020 mM eosin Y, while the others contained cationic dyes: 0.010 mM ethyl violet (EV) and 0.010 mM methylene blue (MB). All of them were treated with 0.4% of the CaC_2O_4-only and CaC_2O_4/BPR inclusion materials. The color change in each supernatant was compared with that of the corresponding dye solution. As a representative cationic dye, EV was selected as the adsorbate for investigating the adsorption mechanism of inclusion material. Into a series of 10-ml solutions with 1.0, 2.0, 3.0, 4.0, 5.0, 6.0, 8.0, 10.0, 12.5, and 15.0 μM EV, 1.5 mg of the inclusion material powder was added. After mixing for 20 min, the liquids were centrifuged at 11,000 rpm for

20 min and the content of EV in the supernatants was determined at 596 nm. By this way, the mole number (γ) of EV binding to the inclusion material was calculated. According to the same method, γ of EV binding to the CaC_2O_4-only material was calculated. Effects of pH from 2.8 to 9.3 and electrolyte from 0 to 1 M were investigated with regard to the adsorption of EV. In addition, the adsorption of EV to powder activated carbon (800–1,000 m^2/g) was determined.

2.2.2 Adsorption of heavy metals

BPR is still one typical complexing agent for heavy metals and, therefore, the CaC_2O_4/BPR inclusion material was tested to adsorb heavy metals. Into a series of heavy-metal mixed solutions with the same composition of 28.2 mg/l Zn^{2+}, 5.96 mg/l Pb^{2+}, 10.8 mg/l Cd^{2+}, 11.0 mg/l Ni^{2+}, and 11.1 mg/l Cu^{2+}, the inclusion material were added from 0 to 5% (w/w). After mixing for 20 min and stewing for 1 h, the concentrations of heavy metals in the supernatants were determined by ICP-OES (Rezić and Steffan 2007). Their adsorption amounts were calculated as well. According to the same method, the adsorption of heavy metals on CaC_2O_4-only material was performed as well. Effect of pH from 4 to 9 on the adsorption of heavy metals was investigated. The adsorptions of Pb^{2+} from 0 to 5,600 mg/l and Cd^{2+} from 0 to 570 mg/l were carefully examined by using 1% of the CaC_2O_4-only and CaC_2O_4/BPR inclusion materials as sorbents.

2.2.3 Treatment of wastewaters

The MB and malachite green (MG) dye wastewater samples (W1 and W2) with 210 (W1) and 207 (W2) of colority were collected from two dyeing mills. Two wastewater samples containing heavy metals (W3 with high Zn^{2+} and W4 with high Cd^{2+}) were collected from two electroplating plants. The pH of all wastewater samples were between 5 and 8. The results from ICP-OES showed that sample W3 contained 294 mg/l Zn^{2+}, 2.14 mg/l Pb^{2+}, 9.91 mg/l Cd^{2+}, 12.0 mg/l Ni^{2+}, and 1.29 mg/l Cu^{2+}, while sample W4 contained 3.35 mg/l Zn^{2+}, 22.9 mg/l Cd^{2+}, 2.31 mg/l Ni^{2+}, 6.23 mg/l Cu^{2+}, and 0 mg/l Pb^{2+}. Ten milliliters of each dye wastewater sample was treated with the CaC_2O_4/BPR inclusion material ranging from 0%, 0.1%, 0.2%, 0.3%, 0.4%, 0.6%, 0.8%, and 1.0%. After mixing for 20 min and stewing for 1 h, the supernatants were determined spectrophotometrically at 637 (W1) and 616 nm (W2). With the same method, 10 ml of each electroplating wastewater sample was treated with 3% of the CaC_2O_4/BPR inclusion material and the contents of heavy metals in the supernatant were then analyzed by ICP-OES.

3 Results and discussion

3.1 Effects of Ca^{2+} and the addition subsequences of reactants

Curves 1–8 in Fig. 1a show the absorption spectra of the BPR solutions containing 10 mg/l $C_2O_4^{2-}$ and various Ca^{2+} concentrations between 1.0 and 50 mg/l according to the addition subsequence: ethanol–$C_2O_4^{2-}$–BPR–Ca^{2+}, in which ethanol may slow down the growth of CaC_2O_4 colloids and refine the particles (Gao 1992). Curves 4–7 depict the light-absorption spectra, with the peak of the complex located at 618 nm. From the curve in Fig. 1b, the peak-valley absorbance difference between 618 and 566 nm remains almost maximal between 100 and 300 mg/l Ca^{2+}. Thus, $C_2O_4^{2-}$ is precipitated completely when Ca^{2+} concentration is over ten times that of $C_2O_4^{2-}$. Therefore, the optimal mass ratio of Ca^{2+} to $C_2O_4^{2-}$ is between 10 and 30. Curves in Fig. 1c show the effects of three addition sequences of reactants on the absorption spectra. By comparison, the third addition subsequence: $C_2O_4^{2-}$–Ca^{2+}–BPR gives the smallest peak-valley absorbance difference. The reason is that CaC_2O_4 particles might have been formed before the addition of BPR. BPR was adsorbed only onto the colloidal electric double layers at the outer surface of CaC_2O_4 particles. The second addition subsequence: Ca^{2+}–BPR–$C_2O_4^{2-}$ achieved a larger peak-valley absorbance interval than the third subsequence. The CaC_2O_4 particles formed rapidly as Ca^{2+} remained in a high concentration (200 mg/l). Thus, there was not sufficient time for BPR to bind onto the
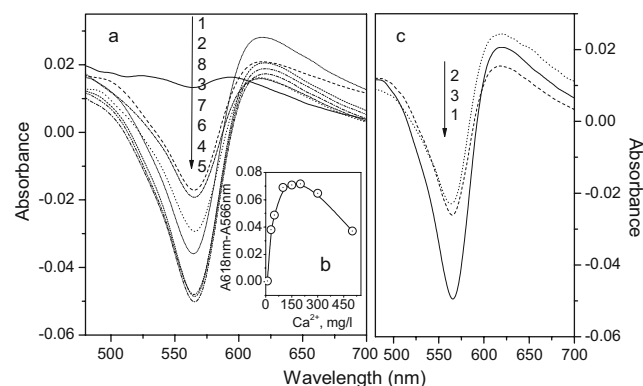

Fig. 1 **a** Absorption spectra of reactions of $C_2O_4^{2-}$ (10.0 μg/ml), BPR (0.010 μmol/ml) and Ca^{2+} (20.0 μg/ml) from 1 to 8: 10.0, 30.0, 50.0, 100, 150, 200, 300, and 500 mg/l in the addition subsequence $C_2O_4^{2-}$–BPR^{2-}–Ca^{2+}. **b** Change of the absorbances' difference of the above solutions between 618 and 566 nm. **c** The absorption spectra of the three addition sequences. 1 ethanol–$C_2O_4^{2-}$–BPR–Ca^{2+}, 2 ethanol–Ca^{2+}–BPR–$C_2O_4^{2-}$, 3 ethanol–$C_2O_4^{2-}$–Ca^{2+}–BPR, where the solutions contain 40% ethanol, 10.0 μg/ml $C_2O_4^{2-}$, 0.010 μmol/ml BPR, and 200 mg/l Ca^{2+}

growing CaC_2O_4 particles. When Ca^{2+} was added in the first subsequence, the slow growth of CaC_2O_4 particles is favorable for BPR to be embedded in layer-by-layer. In addition, effect of electrolyte on the embedment of BPR was also examined. γ of BPR decreased with increasing ionic strengths (Supporting information online Fig. S1). The possible reason is that the electrolyte, e.g. Na^+, is adsorbed competitively on the CaC_2O_4 particles in place of Ca^{2+}. Thus, electrolyte affected the growth of BPR/ CaC_2O_4 inclusion particles.

3.2 The BPR-CaC_2O_4 binding

The complexation among BPR, Ca^{2+}, and $C_2O_4^{2-}$ may be expressed as:

$$N\,\mathbf{BPR}^- + \mathbf{Ca^{2+}} + \mathbf{C_2O_4^{2-}} \overset{K}{\rightleftharpoons} \mathbf{CaC_2O_4(BPR)}_N$$
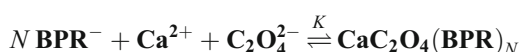
Initiation $\quad {}^c\mathbf{L}0 \qquad\qquad {}^c\mathbf{M}0 \qquad\qquad 0$

Equilibrium $\quad {}^c\mathbf{L} \qquad\qquad {}^c\mathbf{M} \to 0 \quad {}^c\mathbf{M}0$

The symbol N is the saturating number of BPR and K is the adsorption constant (M^{-1}). Both c_{L0} and c_{M0} are the initial molar concentrations of BPR and $C_2O_4^{2-}$, while c_L and c_M represent their molar concentrations at equilibrium. c_M approaches zero when the molar concentration of Ca^{2+} is much higher than that of $C_2O_4^{2-}$. The number (γ) of BPR binding to CaC_2O_4 is calculated by the relation below:

$$\gamma = \eta \times \frac{c_{L0}}{c_{M0}} \tag{1}$$

where

$$\eta = \frac{c_{Lo} - c_L}{c_{L0}} \tag{2}$$

The symbol η is the effective fraction of BPR binding to CaC_2O_4. With increasing BPR concentration, γ approaches N. By comparing curves 1 and 2 in Fig. 2a, γ of BPR adsorbing on CaC_2O_4 particles prepared according to the third addition sequence (see Fig. 1c) is less than that included in CaC_2O_4 particles prepared according to the first addition sequence. Thus, BPR was probably included into the CaC_2O_4 particles to form a supramolecular inclusion material. From curve 2, the optimal BPR addition is between 30 and 50 µM, i.e. the suitable initial molar ratio of $C_2O_4^{2-}$ to BPR is approximately 3. From curves in Fig. 2b, plots γ^{-1} vs. c_L^{-1} fitted the Langmuir isothermal equation:

$$\frac{1}{\gamma} = \frac{1}{N} + \frac{1}{KNc_L} \tag{3}$$

The binding of BPR to CaC_2O_4 corresponds to the chemical adsorption in a monolayer manner. From the intercepts of curves (see Fig. 2b), Ns of BPR to the two kinds of CaC_2O_4 particles were calculated to be 0.0065 ± 0.004 and 0.0105 ± 0.003. The supramolecular complex $[(CaC_2O_4)_m(BPR)]_n^{2n-}$ ($m=95\pm3$) could be formed, i.e. 1 BPR molecule binds to 95 CaC_2O_4 molecules, in which approximately 40% BPR was included into the inner CaC_2O_4 particles. The adsorption constants of the supramolecular complexes were calculated to be $K=3.22\times10^5$ and 4.70×10^5 M^{-1} from the slopes and intercepts of curves 1 and 2. Therefore, the BPR/CaC_2O_4 inclusion complex is more stable than the BPR/CaC_2O_4 surface-binding complex. The embedment of BPR into CaC_2O_4 layers was confirmed. The most possible embedment process of BPR is analyzed as follows. The BPR with sulfonic groups may be adsorbed into the temporary electric double layer by the affinity with Ca^{2+} during the growth of CaC_2O_4 particles. Immediately, $C_2O_4^{2-}$ captured the Ca^{2+} to form the CaC_2O_4 outer enclosed sphere. Thus, BPR can be released and embedded as a sandwich between CaC_2O_4 layers.

3.3 Composition, size, and pattern of the particles

As is well known, recycling and reuse of waste is long studied as a topic in order to conserve the environment and save cost (Liu et al. 2008). A BPR wastewater was used instead of the BPR reagent to synthesize the inclusion material according to the same procedures. The content of BPR/CaC_2O_4 inclusion material in the product liquid was determined to be 10%. The mole ratio of Ca^{2+}, $C_2O_4^{2-}$, and BPR in the three materials were determined: $C_2O_4^{2-}$–Ca^{2+} is 1:1.05 in the CaC_2O_4-only particles, $C_2O_4^{2-}$–Ca^{2+}–BPR is 1:1.06:0.0043 in the BPR/CaC_2O_4 surface-modifying material and 1:0.999:0.0056 in the BPR/CaC_2O_4 inclusion material, respectively. The addition of BPR did not affect the ratio of Ca^{2+} to $C_2O_4^{2}$, which almost remained constant at 1:1. Thus, only one BPR molecule was included into 180 CaC_2O_4 molecules in the inclusion material prepared with BPR dye wastewater. Such an N value is less than that obtained with the diluted BPR standard solution, given that some other organic substances such as unreacted reactants or unknown by-products might exist in the dye wastewater. Another point is that the inclusion complexation was purposely conducted in a solution with highly concentrated $C_2O_4^{2-}$ and Ca^{2+}. This is, to simulate the situation that might be encountered more frequently when treating real industrial wastewaters.

The size distributions of the CaC_2O_4-only and BPR/ CaC_2O_4 inclusion particles were measured (Supporting information online Fig. S2). The CaC_2O_4-only particles are between 0.2 and 1.4 µm (diameter) and their particle sizes are highly non-uniform. Over 80% of the inclusion particles are between 0.7 and 1.02 µm. This indicates that the addition of BPR controlled the aggregation of CaC_2O_4

Fig. 2 Plots γ vs. c_{L0} (**a**) and γ^{-1} vs. c_L^{-1} (**b**) of the solutions containing 40% ethanol, 10.0 μg/ml $C_2O_4^{2-}$ and 200 μg/ml Ca^{2+}. 1-BPR form 0 to 0.025 mmol/l, prepared according to the third addition sequence and 2-BPR form 0 to 0.050 mmol/l, prepared according to the first addition sequence
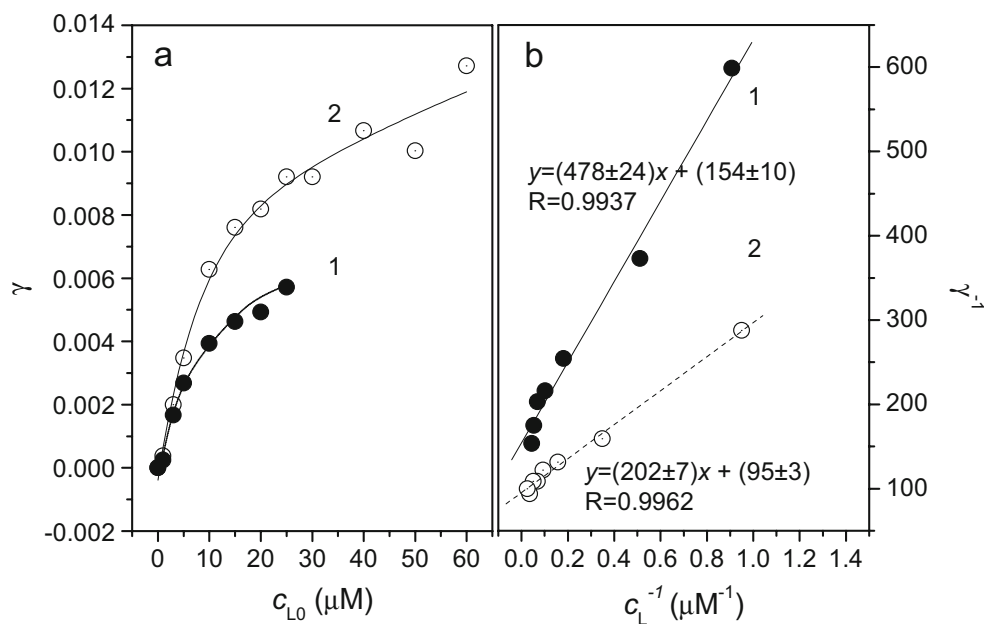
particles to form the size-uniform supramolecular complex. The CaC_2O_4-only grains have fuzzy borderline and globe-like shape with a wide range of sizes between 10 and 60 nm. On the contrary, the CaC_2O_4/BPR inclusion grains are global in 30–50 nm of diameter and their borderlines are very clear. Such differences suggest that the addition of BPR altered the surface structure of CaC_2O_4 particles. In addition, close inspection of the XRD data (Supporting information online Fig. S3) indicates that the mixing of BPR did not alter the crystallization process and crystal-cell shape of CaC_2O_4 particles.

3.4 Adsorption of cationic dyes

The adsorption effect of four dye solutions were carried out: reactive brilliant red, eosin Y, EV, and MB, treated with the CaC_2O_4-only and the CaC_2O_4/BPR inclusion materials. The two cationic dyes were hardly adsorbed (Supporting information online Fig. S4). Similarly, EV and MB were hardly adsorbed on the CaC_2O_4-only material. In contrast, removal of EV and MB are significant when they were treated with the CaC_2O_4/BPR inclusion material. Thus, the adsorption of dye is mainly due to the ion-pair interaction. In a cationic solution, the valence electrons of BRP included in the particles may shift towards the surface of particles via the electrostatic induction and eventually transform them into negatively charged particles (Zhao et al. 2005). Therefore, the CaC_2O_4/BPR inclusion material may be able to adsorb cationic dyes selectively, but repulse all anionic dyes.

The adsorption of EV was investigated in detail with the CaC_2O_4-only and CaC_2O_4/BPR inclusion material and activated carbon. The results are shown in Fig. 3a. From

curve 1, γ of EV binding to the CaC_2O_4-only material is always less than that in the inclusion material. Moreover, γ of EV on activated carbon is less than that on the inclusion material, as seen by comparing curves 2 and 3. From curves in Fig. 3b, the binding of EV to these materials fitted the Langmuir isothermal model. Therefore, all the adsorption of EV corresponded to the chemical adsorption in a monolayer manner. From the intercept and intercept of plots γ^{-1} vs. c_L^{-1}, the saturating numbers (N) of EV and the adsorption constant (K) were calculated as listed in Table 1. From the data of N, the CaC_2O_4/BPR inclusion material adsorbed EV over three times more efficiently than the CaC_2O_4-only particles and two times more than the activated carbon. Thus, the inclusion of BPR largely enhanced the adsorption performance. The 0.0093 of difference (ΔN) (i.e. $\Delta N=0.013-0.0037$) must therefore result from the doping of BPR into the CaC_2O_4 particles. Thus, only one BPR molecule bound with one EV molecule. From the dissociation constant (K_a) of BPR, $pK_{a1}=4.39$, $pK_{a2}=9.13$, and $pK_{a3}=11.27$, univalent BPR^- was formed in neutral media. Therefore, the adsorption of such a sorbent is mainly due to the ion-pair attraction between EV and BPR. From K values, the binding of EV to activated carbon is strongest, but the release of EV from activated carbon may be difficult. From Table 1, the adsorption of EV on the CaC_2O_4-only and CaC_2O_4/BPR inclusion materials was complete in only 5 min at room temperature and the sedimentation of sorbents complete in 1 h. However, that of EV onto activated carbon are much slower than the CaC_2O_4/BPR sorbent.

The effects of pH and ionic strength on the adsorption of EV were investigated using the CaC_2O_4-only and CaC_2O_4/BPR inclusion materials as the sorbents. γ of EV increased

Fig. 3 Plots γ vs. c_{L0} (**a**) and γ^{-1} vs. c_L^{-1} (**b**) of EV. 1-CaC$_2$O$_4$-only, 2-CaC$_2$O$_4$/BPR inclusion sorbent and 3-powder activated carbon
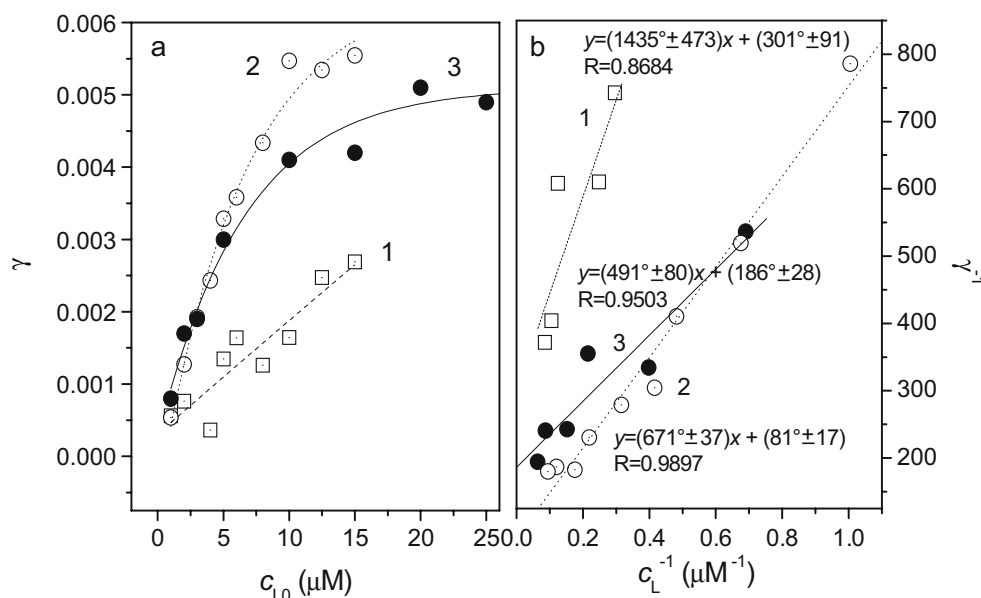
with increasing pH from 5 to 9 and electrolyte concentration (Supporting information online Fig. S5). Therefore, the CaC$_2$O$_4$/BPR inclusion material is more suitable for treating the neutral and alkaline aqueous media with the exception of those containing high salt concentrations.

3.5 Adsorption of heavy metals

As is well known, BPR is still one typical complexing agent for heavy metals, so the CaC$_2$O$_4$/BPR inclusion material was tested to adsorb heavy metals. The removal rates of Zn^{2+}, Pb^{2+}, Cd^{2+}, Ni^{2+}, and Cu^{2+} in various additions of CaC$_2$O$_4$-only and CaC$_2$O$_4$/BPR inclusion materials were calculated (Supporting information online Fig. S6A). Over 90% of Pb^{2+} was removed when the two materials were added more than 0.5%. Thus, CaC$_2$O$_4$ itself can adsorb plenty of Pb^{2+} via the complexation with C$_2$O$_4^{2-}$.

The adsorptions of Cu^{2+} have an apparent difference between the two materials. This indicates that BPR has hardly reacted with Cu^{2+}. Five percent CaC$_2$O$_4$ material adsorbed only 27% Zn^{2+}, 63% Cd^{2+}, and 35% Ni^{2+}, which was unsatisfactory in terms of removal rates. However, the removal rates of Zn^{2+}, Cd^{2+}, and Ni^{2+} increased to 71, 97 and 79% when 5% CaC$_2$O$_4$/BPR inclusion material was used instead. Therefore, such an inclusion material is more effective for treating wastewaters with high concentrations of Pb^{2+} or Cd^{2+}, e.g. electroplating wastewater. The effect of pH on the adsorption of heavy metals to the inclusion material was determined (Supporting information online Fig. S6B). The removal rates of heavy metals, particularly Pb^{2+} and Zn^{2+}, decrease when pH is lower than 5. It is attributed to the fact that the increasing CaC$_2$O$_4$ solubility caused the stripping of BPR into the solution. Hence, such a material may be more effective for treating neutral pH and alkaline wastewaters.

The adsorption of Pb^{2+} and Cd^{2+} was investigated in detail to understand the adsorption mechanism of the CaC$_2$O$_4$-only and CaC$_2$O$_4$/BPR inclusion materials used. Figure 4a shows that 1% of the two materials adsorbed various amounts of Pb^{2+} and Cd^{2+}. Same as the above analysis, the contribution rate of BPR is negligible in the removal of Pb^{2+} by comparing curves 1 and 2, i.e. CaC$_2$O$_4$ itself adsorbed plenty of Pb^{2+}. By comparing curves 3 and 4, BPR complexation is obvious in the removal of Pb^{2+} and the contribution rate is over 50%. The mole masses of Pb^{2+} and Cd^{2+} binding with BPR were calculated by the differences between curves 1 and 2 and curves 3 and 4, as shown in Fig. 4b. Both mole ratios of Pb^{2+} and Cd^{2+} binding to BPR almost remain constant at 1:1 when Pb^{2+} is

Table 1 Determination of adsorption constants of three kinds of sorbents with EV as the absorbate

Sorbents	N of EV, mol/(mole CaC$_2$O$_4$)	K, ×10^5 M^{-1}	Equilibrium/sedimentation time (min/h)
CaC$_2$O$_4$-only	0.0037±0.0011	2.1±0.6	5/1
CaC$_2$O$_4$/BPR inclusion	0.013±0.003	1.2±0.1	5/1
Powder activated carbon	0.0055±0.0008[a]	3.8±0.6	100/5

[a] mol/(mole carbon)

Fig. 4 Adsorptions of Pb^{2+} and Cd^{2+} with 1% CaC_2O_4-only (**a**1 and **a**3) and 1% CaC_2O_4/BPR inclusion material (**a**2 and **a**4). **a** Change of the equilibrium mass (in 10 ml of solution) of Pb^{2+} (1 and 2) and Cd^{2+} (3 and 4). **b** Change of the molar ratios of Pb^{2+} (1) and Cd^{2+} (2) binding to BPR
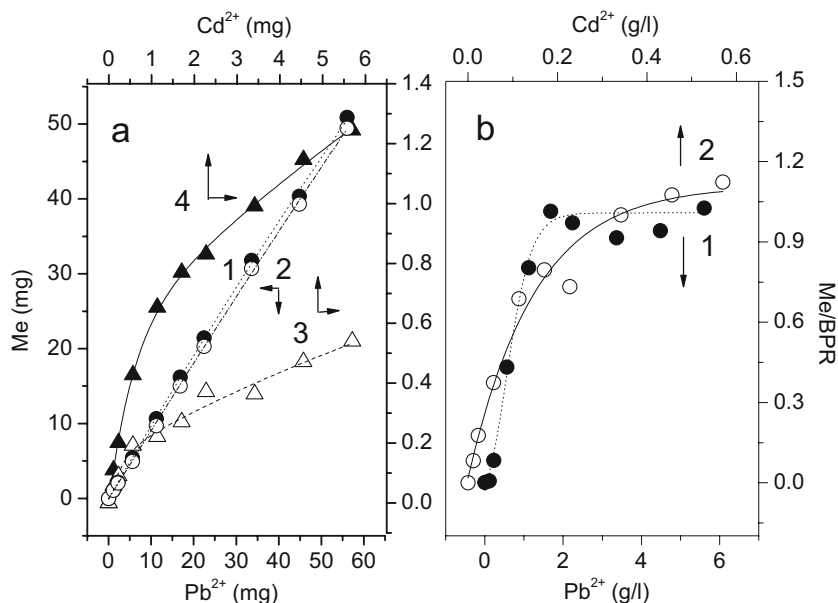
more than 1.5 g/l and Cd^{2+} more than 0.3 g/l. Therefore, BPR plays a vital role in complexing with heavy metals and the CaC_2O_4/BPR inclusion material is demonstrated to be feasible and effective for removing heavy metals.

3.6 Treatment of wastewaters

Two dye wastewater samples (W1 and W2: MB and MG as the raw materials) and two electroplating wastewater samples (W3 and W4) were treated with the CaC_2O_4/BPR inclusion material. After the suspending substances were separated, samples W1 and W2 were analyzed. The decolorization of W1 and W2 are more than 80% when the CaC_2O_4/BPR inclusion material is more than 0.3% added in W1 and 0.7% added in W2 (Supporting information online Fig. S7A). From the color change from W1 to R1 and W2 to R2, where only 0.4% of the inclusion material were added, the inclusion material results in an obvious decolorization effect. As a sludge disposal reuse method, the sludge produced is potentially as the color additive used in building materials, paper-making, plastic, and rubber industries.

From the removal rates of heavy metals with varying concentrations in W3 and W4 (Supporting information online Fig. S7B), treated with 3% of the inclusion material. Regarding W1, 90% of Pb^{2+} was adsorbed, but only 20–25% of Zn^{2+} and Ni^{2+} were removed, corresponding to the above phenomenon. The removal rates of Cd^{2+} and Cu^{2+} are over 50%. By comparing the removals of standard heavy metals solution above (Supporting information online Fig. S6A), the removal rates of Pb^{2+} and Cd^{2+} in wastewaters decreased significantly. Most Zn^{2+} removal resulted from the complexation with BPR at 3% of the inclusion material. Zn^{2+} concentration in the wastewater is

so high that its complexation over-consumed BPR molecules included in the material. For the treatment of W4 with low Zn^{2+} and zero Pb^{2+} content (Supporting information online Fig. S7B), the removal rates of Cu^{2+}, Ni^{2+}, and Cd^{2+} are significantly higher than those of W1. Therefore, the inclusion of BPR into CaC_2O_4 particles is effective for the removal of heavy metals. The sludge produced may be dissolved in strongly acidic media to release the heavy metals for extraction and recovery.

4 Conclusions

By characterizing the $C_2O_4^{2-}$–BPR–Ca^{2+} material using various modern instruments, the ternary in situ embedment electronegative particle $[(CaC_2O_4)_{95}(BPR)]_n^{2n-}$ was synthesized. It is selective, rapid, and high-effective for adsorbing cationic dyes and heavy metals. The adsorption is hardly subject to the impact of electrolyte. With the same method, we may prepare some particular functional materials by embedding the particularly structural ligand, to recover the valuable substances from seriously polluted wastewaters. This work provides a simple method for preparing the highly effective adsorbents by the chemical coprecipitation. If a concentrated BPR wastewater was reused as the inclusion reactant, the sorbent formed is cost-effective. Without doubt, it may play an important role in the 'using waste treat waste' aspect in the near future.

References

Antoniadis V, Tsadilas CD, Ashworth DJ (2007) Monometal and competitive adsorption of heavy metals by sewage sludge-amended soil. Chemosphere 68:489–494

Chatterjee D, Dasgupta S (2005) Visible light induced photocatalytic degradation of organic pollutants. J Photochem Photobiol C Photochem Rev 6:186–205

Chen JS, Liu MC, Zhang JD, Xian YZ, Jin LT (2003) Electrochemical degradation of bromopyrogallol red in presence of cobalt ions. Chemosphere 53:1131–1136

Chen JY, Zhu DQ, Sun C (2007) Effect of heavy metals on the sorption of hydrophobic organic compounds to wood charcoal. Environ Sci Technol 41:2536–2541

Donlagic J, Levec J (1998) Comparison of catalyzed and noncatalyzed oxidation of azo dye and effect on biodegradability. Environ Sci Technol 32:1294–1302

Gao HW (1992) Determination of Ca^{2+} in natural water by dual-wavelength spectrophotometry. Shanghai Environ Sci 11(8):28–29

Gong RM, Li M, Yang C, Sun YZ, Chen J (2005) Removal of cationic dyes from aqueous solution by adsorption on peanut hull. J Hazard Mater B 121:247–250

González M, Mingorance MD, Sánchez L, Peña A (2008) Pesticide adsorption on a calcareous soil modified with sewage sludge and quaternary alkyl-ammonium cationic surfactants. Environ Sci Pollut Res 15:8–14

Hassouna MEM, Elsuccary SAA (2002) Determination of oxalate based on its enhancing effect on the oxidation of Mn(II) by periodate. Talanta 56:193–202

Janos P (2003) Sorption of basic dyes onto iron humate. Environ Sci Technol 37:5792–5798

Jiang SY, Hong Y, Zhou RF, Gao TY (2006) Pretreatment of dye wastewater by electrolysis process. J Tongji Univ Nat Sci 34:638–641

Kadirvelu K, Karthika C, Vennilamani N, Pattabhi S (2005) Activated carbon from industrial solid waste as an adsorbent for the removal of Rhodamine-B from aqueous solution kinetic and equilibrium studies. Chemosphere 60:1009–1017

Laasri L, Khalid Elamrani M, Cherkaoui O (2007) Removal of two cationic dyes from a textile effluent by filtration-adsorption on wood sawdust. Environ Sci Pollut Res 14:237–240

Li Y, Xi DL (2004) Decolorization and biodegradation of dye wastewaters by a facultative-aerobic process. Environ Sci Pollut Res 11:372–377

Liu W, Huang F, Liao Y, Zhang J, Ren G, Zhuang Z, Zhen J, Lin Z, Wang C (2008) Treatment of Cr^{VI}-containing $Mg(OH)_2$ nano-waste. Angew Chem Int Ed 47:5619–5622

Mall ID, Srivastava VC, Agarwal NK, Mishra IM (2005) Adsorptive removal of malachite green dye from aqueous solution by bagasse fly ash and activated carbon-kinetic study and equilibrium isotherm analyses. Colloid Surf A 264:17–28

Maloney JP, Halbower AC, Fouty BF, Fagan KA, Balasubramaniam V, Pike AW, Fennessey PV, Moss M (2000) Systemic absorption of food dye in patients with sepsis. New Engl J Med 343:1047–1049

Mane VS, Mall ID, Srivastava VC (2007) Use of bagasse fly ash as an adsorbent for the removal of brilliant green dye from aqueous solution. Dyes Pigm 73:269–278

McMullan G, Meehan C, Conneely A, Kirby N, Robinson T, Nigam P, Banat IM, Marchant R, Smyth WF (2001) Microbial decolourisation and degradation of textile dyes. Appl Microbiol Biotechnol 56:81–87

Mohanty K, Naidu JT, Meikap BC, Biswas MN (2006) Removal of crystal violet from wastewater by activated carbons prepared from rice husk. Ind Eng Chem Res 45:5165–5171

Moosvi S, Kher X, Madamwar D (2007) Isolation characterization and decolorization of textile dyes by a mixed bacterial consortium JW-2. Dyes Pigm 74:723–729

Noroozi B, Sorial GA, Bahrami H, Arami M (2007) Equilibrium and kinetic adsorption study of a cationic dye by a natural adsorbent—silkworm pupa. J Hazard Mater B 139:167–174

Potapova I, Mruk R, Hübner C, Zentel R, Basché T, Mews A (2005) CdSe/ZnS nanocrystals with dye-functionalized polymer ligands containing many anchor groups. Angew Chem Int Ed 44:2437–2440

Rezić I, Steffan I (2007) ICP-OES determination of metals present in textile materials. Microchem J 85:46–51

Scancar J, Milacic R, Benedik M, Bukovec P (2000) Determination of trace elements and calcium in bone of the human iliac crest by atomic absorption spectrometry. Clin Chim Acta 293:187–197

Sciban M, Radetic B, Kevresan D, Klasnja M (2007) Adsorption of heavy metals from electroplating wastewater by wood sawdust. Bioresource Technol 98:402–409

Senthilkumaar S, Porkodi K (2005) Heterogeneous photocatalytic decomposition of crystal violet in UV-illuminated sol-gel derived nanocrystalline TiO_2 suspensions. J Colloid Interf Sci 288:184–189

Sudipta C, Sandipan C, Bishnu PC, Akhil RD, Arun KG (2005) Adsorption of a model anionic dye, eosin Y, from aqueous solution by chitosan hydrobeads. J Colloid Interf Sci 288:30–35

Tuzen M, Citak D, Soylak M (2008) 5-Chloro-2-hydroxyaniline–copper(II) coprecipitation system for preconcentration and separation of lead(II) and chromium(III) at trace levels. J Hazard Mater 158:137–141

van der Zee FP, Bisschops IAE, Lettinga G, Field JA (2003) Activated carbon as an electron acceptor and redox mediator during the anaerobic biotransformation of azo dyes. Environ Sci Technol 37:402–408

Wang BS, Huang JL, Zhang J (2005) Oxidation of reactive dye wastewater with Fenton reagent. J Harbin Institute Technol 37:1280–1282

Wolfe TA, Demirel T, Baumann ER (1986) Adsorption of organic pollutants on montmorillonite treated with amines. Water Pollut Contr Ted 58:68–76

Yue QY, Li Q, Gao BY, Wang Y (2007) Kinetics of adsorption of disperse dyes by polyepicholorohydrin-dimethylamine cationic polymer/bentonite. Sep Purif Technol 54:279–290

Zhao SX, Castle GSP, Adamiak K (2005) Comparison of conduction and induction charging in liquid spraying. J Electrostat 63:871–876

Zhu LZ, Hu JZ, Shen XQ, Cha J (1995) Organobentonites as adsorbents for p-nitrophenol and its application in water treatment. Acta Sci Circumstantiae 15:316–321